Multi-Objective Optimization of 400 kV Composite Insulator Corona Ring Design

BENALIA M'HAMDI[1], YOUCEF BENMAHAMED[2], (Member, IEEE), MADJID TEGUAR[2], IBRAHIM B. M. TAHA[3], AND SHERIF S. M. GHONEIM[3], (Senior Member, IEEE)

[1]Applied Automation and Industrial Diagnostics Laboratory (LAADI), Ziane Achour University of Djelfa, Djelfa 17000, Algeria
[2]Laboratoire de Recherche en Electrotechnique, Ecole Nationale Polytechnique, El Harrach, Algiers 16200, Algeria
[3]Department of Electrical Engineering, College of Engineering, Taif University, Taif 21944, Saudi Arabia

Corresponding author: Sherif S. M. Ghoneim (s.ghoneim@tu.edu.sa)

ABSTRACT The electric field distribution is one of the main factors governing the long-term reliability of high voltage composite insulators. However, under severe pollution conditions, electric field stresses, when exceeding thresholds and applying for long periods, could lead to degradation and deterioration of the housing materials and, therefore, to failures of the composite insulators. This paper is intended to improve the distributions of the electric field and potential by minimizing the corona ring on a 400 kV AC transmission line composite insulator. The performances of three powerful multi-objective meta-heuristic algorithms, namely Ant Lion Optimizer (MOALO), Particle Swarm Optimizer (MOPSO), and non-dominated sorting genetic algorithm (NSGA-II) are established to achieve this goal. First, variations of electrical fields on the critical parts of the string are obtained using three-dimensional finite element method (FEM) software. Then, three objective functions are developed to establish the relationships between the electric field and the guard ring parameters. Finally, the optimization parameters consist of diameter, tube diameter, and installation height of the corona ring. The obtained results confirm the effectiveness of the three algorithms; the MOLAO is the better in terms of computing time and solution quality.

INDEX TERMS Composite insulator, corona ring, electric field distribution, finite element method (FEM), multi-objective, MOALO, MOPSO, NSGA-II.

I. INTRODUCTION

In front of the expansion of national grids and the connection reasons with the Maghrebian and European networks, the Algerian Electricity and Gas Company (SONELGAZ) needed to develop 400 kV grids [1]. However, such transition of the electrical network to a higher voltage engenders a high electric field. Therefore, this latter should be enhanced to mitigate or even avoid hazardous consequences, whose the most harmful is the "insulators flashover" [2]–[7].

Nowadays, composite insulators are widely used in electrical networks because of their lower price, lighter weight, greater design flexibility, higher mechanical strength, better antipollution performance, and lower maintenance requirements [7]–[10]. However, since they are made up of organic materials, they are subject to possible chemical

The associate editor coordinating the review of this manuscript and approving it for publication was Sotirios Goudos.

changes, erosion, and tracking, leading to the failure of such insulators [10]–[12].

To improve reliability and extend the life of composite insulators, numerous investigators have focused on the optimization of the electric field along the non-ceramic insulator string using, among others, conventional corona rings [7], [12]–[15]. The various studies carried out to reduce the electric field around the insulator's string using the corona ring relate to optimizing its design (diameter and tube radius in particular) and its position [4], [13], [15]–[18].

In real-life, many problems have more than one objective to be optimized. Nevertheless, these objectives could conflict with each other; i.e., an improvement in one objective could lead to the deterioration of at least one of the other objectives. Therefore, there exists a set of optimal compromise solutions called non-dominant or Pareto optimum solutions (Pareto front solutions) for which there is no alternative, in which all the parameters (factors) would be in a better position [19].

Optimization problems could be difficult to solve through conventional methods, especially when, in the presence of multiple constraints, these problems are complex, multi-modal, discrete, or discontinuous [15]. In addition, they sometimes require considerable computing time. There-fore, meta-heuristic algorithms were established for differ-ent kinds of real-life optimization problems to overcome such difficulties [19]–[28]. These algorithms are robust and allow obtaining the global optimum in less computation times. Also, they are easy to implement due to their sim-ple mathematical models and are among the most effective approaches [19]–[22], [25], [26].

Some of the most common evolutionary algorithms con-sist of Genetic Algorithm (GA) [20], Ant Colony Opti-mization (ACO) [21], and Particle Swarm Optimization (PSO) [22]. Other techniques were also developed such as Cuckoo search algorithm (CSA) [23], whale optimization algorithm (WOA) [24], grey wolf optimizer (GWO) [25], ant lion optimizer (ALO) [26], virus colony search (VCS) [27], and dolphin echolocation (DE) [28]. Their effectiveness has been demonstrated in various practical engineering prob-lems. Otherwise, numerical techniques have been devel-oped to optimize HV insulators design by improving the electric field performance. For instance, the Finite Element Method (FEM), which is suiTable for low-frequency appli-cations, remains widely used by high-voltage engineering researchers [1], [29].

In the present investigation, multi-objective versions of GA, PSO, and ALO are proposed to minimize the elec-tric field at 400 kV AC transmission lines composite insulator surface. Including the tower and corona ring, a three-dimensional finite element model is established. The influence of the corona ring parameters, consisting of its diameter, tube radius, and position (height), is analyzed. The electric field at the triple point (HV side) is calculated for ring parameters ranges by changing parameter by parameter. A mathematical model composed of three objective functions is developed based on the obtained results to establish the relationships between the electric field and the ring parame-ters. Optimizing such relationships allows obtaining the ring parameters leading to the lowest electrical field level. For this purpose, three powerful multi-objective meta-heuristic algorithms, namely, Ant Lion Optimizer (MOALO), Parti-cle Swarm Optimizer (MOPSO), and non-dominated sorting genetic algorithm (NSGA-II) are developed. The optimiza-tion results are discussed according to the quality of the solution and the computation time. It is worth noting that multi-objective optimization techniques have never been used in this area so far.

Such techniques generate a multitude of solutions, gen-erally very different. The most representative solutions are kept and the other are rejected. Among the representative solution, the decision marker selects the best one. The greater the difference between the representative solutions, the more difficult the choice is [19], [30], [31]. Such drawbacks are not

TABLE 1. Technical information of composite insulator.

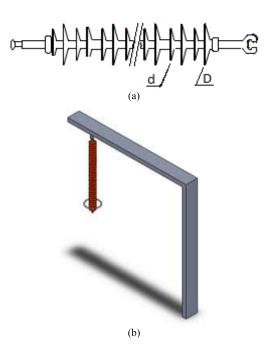| Line Voltage [kV]	400
Leakage distance [mm]	7770
Dry arcing distance [mm]	3105
Insulator length [mm]	3368
Number of Sheds (N/n)	40/40
Sheds diameter D/d [mm]	114/97

FIGURE 1. Real and simplified insulators a) Real composite insulator b) Insulator model used for simulation.

encountered in this study since the solutions we have obtained very close, and choosing the best solution is too easy.

II. COMPUTATION MODEL
For this investigation, a typical 400 kV polymer insulator is used. The insulator is 3368 mm long with 40 large sheds and 40 small sheds. The diameter of large shed is 114 mm while the small's is 97 mm. The insulator is made of silicon rubber weather sheds with a relative permittivity of 4.3, a fiberglass rod with a relative permittivity of 7.2 and metallic fittings. The technical characteristics of the composite insulator are presented in Table 1. Figure 1 shows the non-ceramic insula-tor used in a 400 kV transmission system and the simplified model employed for the simulation. The insulator is vertically suspended. The top metallic end fitting is connected to the tower (the ground electrode), and the bottom one is con-nected to the line (the high voltage electrode) whose voltage is 231 kV (=400 kV/$\sqrt{3}$). A corona ring, which is essentially a toroidal-shaped metal ring, is placed at the energized end side of the insulator, where a high electric field is normally produced. The ring's optimal parameters (the diameter, tube diameter, and vertical position) will later be determined. Sim-ulations have been conducted in clean and dry conditions.

The electric field control is important, especially in three main zones: the polymer weather-shed surface, the interior of the fiberglass rod, and the surfaces of the metal fittings and corona rings. In addition, the electric field stress is more significant at the triple point junction of three media consisting in HV end fitting, polymer, and air [4], [8], [9]. Such a situation may strongly reduce the insulation performance of the insulator.

The corona ring is used to reduce the electric field on the surface of the composite insulators below the threshold values for corona inception in both dry and wet conditions [15], [18].

The electric field distribution on the insulator surface depends not only on the applied voltage level but also on the insulator profile and the corona ring parameters consisting of the diameter D, the tube inner radius r, and the mounting height h.

In this study, the electric field value is evaluated for different values of corona ring parameters since no standards exist for the design and placement of corona rings [15], [18]. Indeed, generic corona ring configurations have been considered with outer diameters ranging from 250 to 550 mm, tube diameter from 30 to 90 mm, and mounting height from 0 to 650 mm. Furthermore, the parameters D, r, and H are varied by steps of 50 mm, 5 mm, and 50 mm, respectively [15].

III. EFFECTS OF CORONA RING PARAMETERS

The corona rings are installed to reduce and improve the distribution of the electric field and consequently reduce the failures appearing in the transmission systems and extend the lifetime of the insulators [14], [15]. Manufacturers suggest the application of corona rings on the active end of the insulators used for more than 230 kV and on both ends for those employed for more than 500 kV. Since, there are no standards for the design and placement of rings, the latter's dimensions vary from one manufacturer to another [14], [15].

The electric field should not exceed 450 kV/m on the sheath for the dry uncontaminated composite insulator and 350 kV/m on the end-fitting seal [4], [10], [14].

Otherwise, the parameters of the corona rings, namely the ring diameter, D, the inner radius of tube, r and the mounting height, H, are taken as decision variables since these parameters considerably affect the electric field [4], [10], [15], [16].

The electric field norm is computed along the central axis of the composite insulator to determine the effect of corona rings parameters on the electric field distribution over the insulator. As explained in previous work [15], the electric field norm at first augments promptly reaches the maximum at the triple point and decreases rapidly.

The effects of the corona ring parameters on the maximum value of the electric field (computed at the triple point) are shown in Figures 2 to 4. Note that the electric field at the triple point is calculated by changing one parameter while the two others are kept constant. The maximum electric field norm
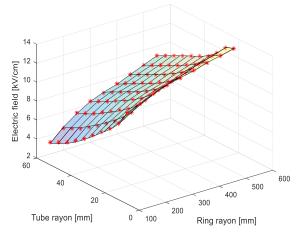

FIGURE 2. Effect of the tube radius and the ring radius on the maximum E field.

strength was significantly decreased when using the corona ring.

Figure 2 depicts the synchronous effect of the ring diameter and the ring tube diameter on the maximum electric field at the triple point. A simultaneous decrease of the ring diameter and increase of the ring tube diameter leads to a significant decrease in the electric field norm. Note that, to avoid any contact between the ring and the large shed, the inferior limit of the corona ring rayon has been chosen, in our investigation, equal to 130 mm.

Figure 3 illustrates the simultaneous effect of the ring tube diameter and the installation height on the maximum electric field at the triple point. The electric field norm of the insulator decreases slightly with increasing the ring tube diameter when the mounting height is in the range of 150mm to 300mm, elsewhere there is no effect and the electric field is practically constant. On the other hand, the electric field norm first decreases significantly when increasing the corona ring mounting height. It reaches a minimum then after before increasing again. The minimum value, corresponding to more than 40% of maximum electric field norm reduction, is obtained approximately for 225 mm mounting height and 60 mm ring tube diameter.

As shown in Figure 4, the maximum electric field at the triple point of the insulator is almost constant for a corona ring radius greater than 400 mm. However, the electric field norm at the triple point decreases significantly when the radius of the corona ring decreases when the mounting height is about 250 mm. For the other corona ring mounting height values, the decrease of the corona ring radius leads to the electric field increase.

IV. CORONA RING OPTIMIZATION PROBLEM FORMULATION
A. MULTI-OBJECTIVE OPTIMIZATION BASIC CONCEPT
In mono-objective optimization, only one global optimum solution is relatively easy to find. However, in multi-objective problems, solutions must be compared to more than
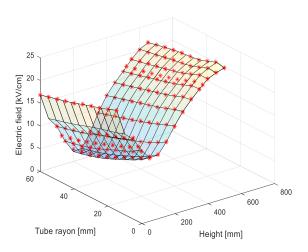
FIGURE 3. Effect of the ring tube radius and the ring height on the maximum E-field.
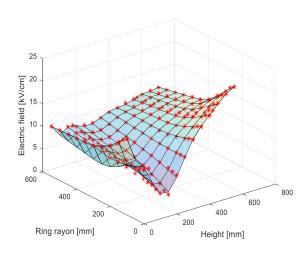

FIGURE 4. Effect of the ring radius and the ring height on the maximum E-field.

one objective (criterion). The multi-objective optimization problem can be mathematically expressed to minimize or maximize multiple objective functions subjected to a set of constraints as follows [19]:

$$\text{Minimize} \quad F(x) = [f1(x), f2(x), \ldots., fn(x)]$$
$$\text{Subject to} \quad gk(x) \le 0, \quad k = 1, \ldots, m,$$
$$xi(L) \le xi \le xi(U), \quad i = 1, 2. \ldots \quad (4.1)$$

where

• x is a vector of d decision variables x = [x1, x2, . . . , xd]T.
• fi(x), i = 1, . . . , n are the objective functions.
• gk(x), k = 1, . . . , m are the constraint functions of the problem.
• xi(L) and xi(U) lower and upper bounds respectively.

According to the Pareto optimality concept, solving a multi-objective problem (MOP) allows obtaining a set of

(possible) best solutions in which one objective cannot be improved without damaging another one. In a minimization problem, Pareto dominance and Pareto optimality are defined as follows:

Pareto dominance: A given vector x = [x1, x2, . . . ,xd] is said to dominate y = [y1, y2, . . . ,yd]

if and only if ∀i∈ {1, 2, . . . ,n}, xi ≤ yi and ∃i∈{1, 2, . . . ,d}, xi <yi.

Otherwise, a given solution is called Pareto optimal if another solution does not dominate it.

B. FORMULATION OF THE OPTIMIZATION PROBLEM (OBJECTIVE FUNCTION)

Based on the above results, the corona ring on the conductor side should have the optimum corona ring configuration to maintain the electrical field intensity on the composite insulator, lower than the threshold value of 450 kV/m to prohibit the discharges activities in particular near the energized end fitting. The optimal configuration is achieved by minimizing the electric field via the multi-objective functions.

Mathematical relations (objectives functions) between the electric field magnitudes and corona ring parameters to fully reflect the electric field distribution of composite insulators. These functions allow us to apply different optimization algorithms to find the optimal corona ring parameters minimizing the electric field.

The polynomial regression approach models the relationship between the independent variables (corona ring parameters) and the dependent variable electric field. The polynomial regression deviations are evaluated based on optimum mean square error (RMSE) and coefficient of determination (R2) values.

The following equations represent the proposed model:

$$E(H, R) = \sum_{i,k} a_{ik} H^i R^k i, \quad k = 0, \ldots, 8 \quad (4.2)$$

$$E(H, r) = \sum_{i,j} a_{ij} H^i r^j i, \quad j = 0, \ldots, 8 \quad (4.3)$$

$$E(r, R) = \sum_{j,k} a_{jk} r^j R^k j, \quad k = 0, \ldots, 8 \quad (4.4)$$

where a_{ik}, a_{ij} and a_{jk} are the polynomial coefficients. R, H and r are the ring diameter, the installation height and the ring tube diameter, respectively.

To obtain a convenient corona ring size, the objective function should be subjected to various constraints defined by the ring parameters' influence ranges. Depending upon performed simulation tests presented in Figures 2 to 4 (corona ring parameters effects) and geometric feasibility, the selected constraints are given as follows:

$$0 \text{ mm} \le H \le 650 \text{mm}$$
$$130 \text{ mm} \le R \le 550 \text{mm}$$
$$15 \text{ mm} \le r \le 60 \text{mm}$$

C. MULTI-OBJECTIVE OPTIMIZATION ALGORITHMS

One might be to find a set of Pareto optimal solutions and/or quantify the trade-offs which can be satisfied in objectives These algorithms allow finding Pareto optimal solutions set and/or quantifying the trade-offs that can be satisfied in the objectives. In this study, three efficient meta-heuristic algorithms, MOALO (Mirjalili 2016) [19], NSGA-II (Deb *et al.* 2002) [30], and MOPSO (Moore and Chapman 1999) [31] are adopted to optimize the corona rings design parameters. The details of the recently proposed multi-objective Ant Lion Optimizer (MOALO) and a very brief description of the two others algorithms are presented in the following subsections.

1) MULTI-OBJECTIVE ANT LION OPTIMIZER (MOALO)

Like all multi-objective algorithms, the Multi-Objective Ant Lion Optimizer starts the optimization process with multiple candidate solutions. These latter are compared with each other using the Pareto dominance operator. The non-dominated solutions are stored in a repository at each iteration, and the algorithm attempts to improve them in subsequent iterations.

The Multi-objective ant lion optimizer (MOALO) is the multi-objective version of the Mono-objective ant lion optimizer (ALO). The ALO algorithm [26] mimics the interaction between Ant Lions and ants in the trap. The ALO approximates the optimal solutions employing random solutions set. This latter is improved applying the principles inspired from the hunting mechanism of Ant Lions and the interaction of their favorites prey (ants) with them. The ants are supposed to move randomly over the search space, and the Ant Lions can use traps and are expected to hunt them to model such interactions.

In their search for food in nature, the ants first wander randomly. Their random walks can be modeled as follows:

$$X(t) = [0, cumsum(2r(t_1) - 1), cumsum(2r(t_2) - 1),$$
$$\ldots, cumsum(2r(t_n) - 1)] \quad (4.5)$$

where cumsum calculates the cumulative sum, n is the maximum number of iterations, t shows the step of random walk, and r(t) is a stochastic function defined as follows:

$$r(t) = \begin{cases} 1 & if \ rand > 0.5 \\ 0 & if \ rand \leq 0.5 \end{cases} \quad (4.6)$$

rand is a random number generated with uniform distribution in the interval of [0,1].

During optimization, an ant position refers to the parameters for a particular solution and position of all ants is saved in the M_{Ant} matrix, and also each Ant Lion position is saved in the $M_{AntLion}$ matrix:

$$M_{Ant} = [A_{ij}] \quad M_{Antlion} = [AL_{ij}] \quad (4.7)$$

where $A_{i,j}(AL_{i,j})$ presents the value of *j-th* variable of *i-th* ant (Ant Lion).

The value for the fitness function of each ant is saved in the matrix MOA and analogously, the values of Ant Lions fitness function are saved in the matrix MOAL:

$$M_{OA} = \begin{bmatrix} f[A_{1,1}, \ldots, A_{1,d}] \\ . \\ . \\ . \\ f[A_{n,1}, \ldots, A_{n,d}] \end{bmatrix}$$

$$M_{Antlion} = \begin{bmatrix} f[AL_{1,1}, \ldots, AL_{1,d}] \\ . \\ . \\ . \\ f[AL_{n,1}, \ldots, AL_{n,d}] \end{bmatrix} \quad (4.8)$$

n and d are the number of ants and the number of variables. Considering that the ants update their positions with a random walk at each optimization stage. So, to keep them inside the search space, they are normalized using the following expression:

$$X_i^t = ((X_i^t - a_i) * (d_i^t - c_i^t) / (b_i - a_i)) - c_i^t \quad (4.9)$$

where a_i and b_i are the minimum and the maximum of random walk in *i-th* variable. Also c_i^t and d_i^t are the minimum and the maximum of *i-th* variable at *t-th* iteration.

The equations describing the trapping in Ant Lion's pits are:

$$c_i^t = Antlion_j^t + c^t$$
$$d_i^t = Antlion_j^t + d^t \quad (4.10)$$

where c^t and d^t are respectively the minima, and the maximum of all variables at *t-th* iteration, of all variables at *t-th* iteration, and *Ant Lion* is the position of the selected *j-th* Ant Lion at *t-th* iteration.

A fitness-proportional roulette wheel selection models the hunting ability of the Ant Lion. The roulette wheel assists fitter Ant Lions to attract more ants. In another way, it consists in adaptively reducing the radius (the boundaries) of the random walking hyper-sphere of the ants. The expressions describing how the trapped ant slides down towards Ant Lion are:

$$c^t = c^t / I$$
$$d^t = d^t / I \quad (4.11)$$

where I is a ratio ($I = 1 + 10^w t/T$), T is the maximum iterations number, and w is a constant set according to the current iteration (w = 2 when t > 0.1T, w = 3 when t > 0.5T, w = 4 when t > 0.75T, w = 5 when t > 0.9T, and w = 6 when t > 0.95T).

The final stage of hunt in ALO consists of a capture of the ant and reconstructing the pit to catch new prey. The formulation of this mechanism is as follows:

$$Antlion_j^t = Ant_j^t \quad if \ f(Ant_j^t) < f(Antlion_j^t) \quad (4.12)$$

where $Antlion_j^t$ and Ant_j^t show the position of selected i-th ant and j-th Ant Lion at t-th iteration.

Finally, elitism is achieved as follows: the best Ant Lion is assumed to be elite in each iteration. Furthermore, it implies that each Ant walks randomly around the selected Ant Lion and possesses the position:

$$Ant_i^t = (R_A^t + R_E^t)/2 \qquad (4.13)$$

R_E^t is the random walk around the elite Ant Lion at the t-th iteration, and R_A^t is the random walk around the Ant Lion selected by the roulette wheel at the same iteration.

MOALO algorithm uses an archive to store Pareto optimal solutions to find and store Pareto optimal solutions. However, finding the Pareto optimal solutions set with a high degree of diversity is hard. Therefore, MOALO utilizes leader selection and archives maintenance to overcome this challenge, inspired by the MOPSO algorithm.

The Ant Lions are selected from the solutions with the least populated locality to improve the archive distribution. Therefore, the probability of choosing a solution in the archive is:

$$P_i = c/N_i \qquad (4.14)$$

When the archive is full, the solutions with the most populated locality are removed to accommodate new solutions. The probability of removing a solution from the archive is defined by:

$$P_i = N_i/c \qquad (4.15)$$

where N_i is the number of solutions close to the i-th solution and c is a constant which should be higher than 1. The basic steps of the MOALO are illustrated in the pseudo-code in Algorithm 1 [19] and the flowchart of Figure 5.

Algorithm 1 Multi-Objective Ant Lion Pseudo-Code
___
Initialize randomly the ants and antlions population
while maximum of generations is not fulfilled
    for each ant
        Randomly pick an antlion from the archive
        From the archive select the elite using Roulette
        wheel
        Upgrade c and d using equations Eq. (4.12)
        Randomize walk and normalize it according to
        Eqs. (4.1) and (4.3)
        Update the ant's position according to Eq. (4.14)
    end for
    determine for all ants the values of the objective function.
    Update archive
    if the archive is complete
        To accommodate new solutions. Delete some solutions from the archive
        using the roulette wheel and equation (4.11)
    end
end while
return the archive
___

2) MULTI-OBJECTIVE PARTICLESWARM OPTIMIZATION (MOPSO)

MOPSO is the multi-objective version of the PSO. It is one of the most popular algorithms in the multi-objective optimization area. The basic principle of the MOPSO algorithm is the initialization and the evaluation of the population and then
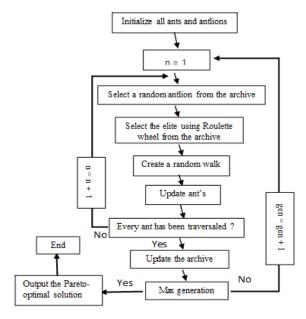

FIGURE 5. Flowchart of MOALO.

repetition of the search by combining PSO operators with Pareto-dominance criteria. In this process, the non-dominated solutions (particles) are archived in repository, and are used to guide the particles search. If the number of solutions exceeds the directory size, they are reduced by using a crowding operation, which is used to crowd the best global solutions considered as leaders. An effective elitist-mutation strategy was also used to maintain the population's diversity and explore the research space more intensively. The basic steps of the MOPSO are summarized within the pseudo-code in Algorithm 2 [32] and in the flowchart of Figure 6.

Algorithm 2 Multi-Objective Particle Swarm Optimization Pseudo-Code
___
Initialize population (position and velocity)
Initialize Archives
Determine Leaders Archive
While iter $\leq$ maxit do
    For all the particles
        Select leader
        Update the position of particles
        Perform mutation
        Evaluation each of the particles (objective function)
        Store the positions of the Pbest particles
    End for
    Update the contents of the archive
    Update the leader's archive
    Increment iteration (iter = iter + 1)
End while
Return Archive
___

3) NON-DOMINATED SORTING GENETICALGORITHM (NSGA-II)

The non-dominated sorting genetic algorithm (NSGA-II) is the multi-objective variant of the genetic algorithm (GA) [20]. In 2002, Deb *et al.* proposed the NSGA-II. They introduced the elitism to enhance the convergence properties
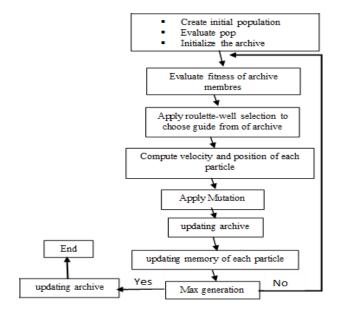
FIGURE 6. Flowchart of MOPSO.

FIGURE 7. Flowchart ofNSGA-II.

and improve the algorithm searches' efficiency and robustness [30]. NSGA-II uses the elitism method for sorting and classifying all individuals and employs a crowding operation to crowd the best global solutions considered leaders for keeping the diversity among the obtained Pareto optimal solutions [30]. The NSGA-II basic steps pseudo-code is summarized in Algorithm 3 and flowchart of Figure 7.

Algorithm 3 Non-dominated Sorting Genetic Algorithm (NSGA-II)

Set parameters
Initialize random Population
Calculate fitness values
Ranking individuals based on Pareto dominance sort
Generate Childs
Apply binary tournament selection and crossover
Perform mutation and recombination
While iter ≤ he max-iter do
    For each child and each parent do
        Create non-dominated fronts sets
        Loop using existing solutions to next generation
        Allocate rank based on Pareto sort
        Find crowding distances
    End for
    Select population from best ranked solutions
    Generate next generation
    Apply binary tournament selection
    Perform mutation and recombination
    Store optimal solutions
End while
Return solutions

V. SIMULATION RESULTS AND DISCUSSION

The three proposed meta-heuristic algorithms (MOALO, MOPSO and NSGA-II) optimize corona ring settings based on the previous mathematical model. It was used to reduce the maximum electrical field at the triple point junction (of three media composed of HV end fitting, polymer, and air) of the composite insulator to accepTable levels.
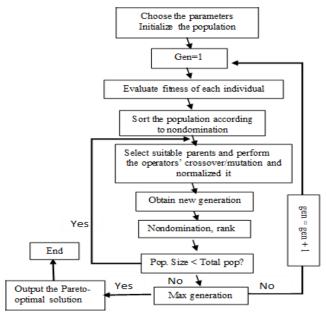
The main criteria to measure the three algorithms ' performance is used to measure the multi-objective functions' best values obtained and the iterations number required to converge. The same initial starting values, obtained from ten randomly selected populations, are used for the three algorithms.

Due to the random factor included in the three algorithms, these latter are run five times and the statistical results are reported. It is noted that all along the five different executions, the three algorithms converge towards the same solution (optimal solution of multi-objective functions). This explains their great stability and robustness in the search for global solutions. Note that for the three algorithms, the common parameters were set at 100 search agents, 250 iterations and an archive size of 100 in the optimization trials. Basing on Design of Experiments (DOE), a sensitive analysis of the MOPSO and the NSGA-II is performed for each algorithm with different combinations of each parameter. The parameter values resulting in better quality solutions are adopted during this analysis. The corresponding parameters are shown in Table 2. Note that there are no parameters of MOALO to be adjusted.

The Inverted Generational Distance (IGD) formulating was used to assess the approximation performance of the algorithms as follows:

$$IGD = \frac{\sqrt{\sum_i^n d_i^2}}{n} \qquad (4.16)$$

where n is the number of solutions of the optimal Pareto true front and d_i indicates the Euclidean distance between each point of the front and the closest member of the approximation.

TABLE 2. Algorithms parameters.

MOALO		
MOPSO	Mutation Rate	0.1
	Inertia Weight	0.5
	Personal and Global Learning Coefficient	c1=1 c2=2
NSGA-II	Mutation Rate	0.02
	Mutation Percentage	0.4
	Crossover Percentage	0.7

TABLE 3. Statistical results of IGD.

IGD	MOALO	MOPSO	NSGA-II
Average	0.03732	0.03810	0.04644
standard deviation	0.001069	0.006231	0.008772

TABLE 4. The optimum solutions, the computation times and the iterations number for the three algorithms.

Algorithm	Number of iterations to convergence	Computational time for convergence	Total computational time	Multi-objective function
MOALO	15	0.8450	25.896	1.8489
MOPSO	10	0.5583	41.20	1.8489
NSGA-II	68	41.7523	236.022	2.1085

The algorithms are run 10 times and the statistical results are presented in Table 3. Since the IDG are very small, the solutions are close to the optimal Pareto front.

From optimal solutions presented by the Pareto fronts in Figures 5 and 6, we present in Table 4 the electric field optimal minimization considered as the optimum (the best) solution for each multi-objective function as well as the number of iterations, the computational time for convergence, and the total computational one.

Although the three algorithms converge towards practically the same result, Table 4 shows that the execution time of the MOALO algorithm is less than the other two algorithms MOPSO and NSGA-II ones, therefore the MOALO converges more quickly. The average time to run only one iteration is 0,0463s for the MOALO against 0, 1218s, and 0,568s for the MOPSO and the NSGA-II. Note that for MOPSO, the run time of an iteration increases during the second half of the total iterations number, while this time is almost the same for all iterations for the other algorithms. Compared to the computation time found by the MOPSO (respectively the NSGA-II), a reduction of about 55% (respectively 75%) has been obtained when using the MOALO.

The Pareto optimal fronts obtained by the three algorithms are presented in Figures 8 and 9. Figure 8 illustrates the plane (f1, f2) of the three-objective optimization Pareto fronts. This Figure shows that the three algorithms spread the solutions differently over the non-dominated front. MOPSO can find a much better distribution than the MOALO algorithm; the
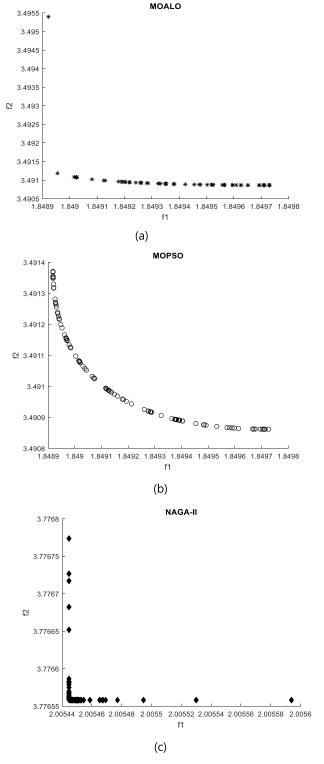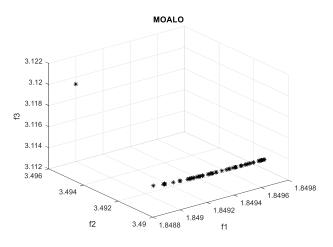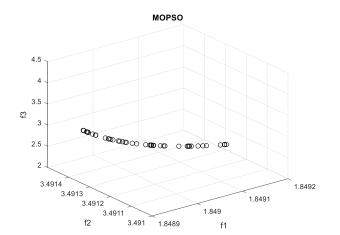

(a)

(b)

(c)

FIGURE 8. Best pareto optimal solution set of the electric field objective functions 1 and 2 according to the multi-objective algorithms MOALO, MOPSO and NSGA-II.

NSGA-II is the worst in spreading the solutions over the non-dominated front.

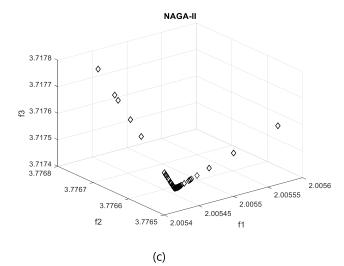Multiple runs of the three algorithms (MOALO, MOPSO and NSGA-II) for the corona ring settings design

(a)

(b)

(c)

FIGURE 9. Three-dimensional pareto optimal solution set of the electric field objective functions 1, 2 and 3 according to the multi-objective algorithms MOALO, MOPSO and NSGA-II.

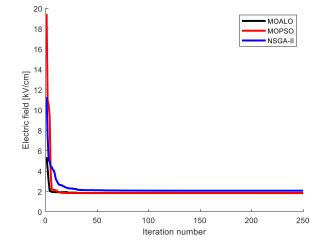optimization generate very sTable Pareto frontiers for each algorithm as shown in Figure 8.

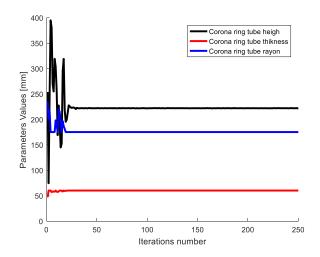**FIGURE 10.** Objective function convergence (electric field).

FIGURE 11. Convergence of the corona ring parameters during the optimization process.

TABLE 5. Optimal corona ring parameters.

Parameters	Corona Ring thikness [mm]	Corona Ring tube Radius [mm]	Corona Ring tube high [mm]	Electric field [kV/cm]
MOALO	60	130	223.634	1.84891
MOPSO	60	130	222.745	1.84893
NSGA-II	57.9978	137	223,607	2.1085

The minimum values reached for the three multi-objective functions on the five different executions of all algorithms are shown in the Figures 10 and 11. The first Figure shows the best solution for the fitness functions, while the second Figure shows the best values for corona ring parameters.

For the three algorithms, the search begins with a high random value. This value obtained for the multi-objective functions, falls rapidly on the first iterations (up to 10) and then a regular decrease thereof before reaching the minimum

TABLE 6. Electric field.

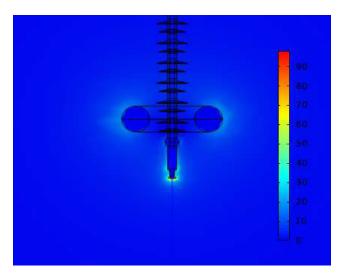| position		Electric field [kV/cm]
Insulator sheds		1.3
Corona ring	Outer radius	11.15
	Inner radius	1

FIGURE 12. Electric field distribution.

value (optimal value). From Figure 10, it is noticeable that both the two algorithms MOALO and the MOPSO converge promptly to the optimal solutions, whereas the NSGA-II cannot converge before the 68 iterations.

As stated above, corona may occur on composite insulator surface, especially at triple junctions where the electric field is more intense. The installation of a corona ring reduces the electric field stress near the HV end fitting. During design, some corona ring parameters must be considered for maximum field stress reduction. The parameters consist of corona ring radius, the radius of the ring tube, and the vertical position of the ring. The results presented in Figure 11 and Table 5 show the electric field's minimum (optimal) value (1.8489 kV/cm) on the insulator shed. The triple point is achieved for 130 mm corona ring diameter, 60 mm corona ring tube radius, and 223 mm corona ring tube height (corona ring position). With such an optimized configuration, the magnitudes of the electric field on the insulator surface sheds and flange, provided in Table 6, are less than the critical value [30].

The electric field distribution on the surfaces of the composite insulator and the corona ring is illustrated in Figure 12 to show the improvement of the electrical field distribution on the surface of the composite insulation due to the use of an optimal corona ring. It is visible that the electrical field is concentrated mainly on the cross-section of sheds close to the energized end and on metal parts. In addition, it should be noted that the electric field magnitude at the inner radius of corona ring is less than at the outer one (Table 6). It is due to
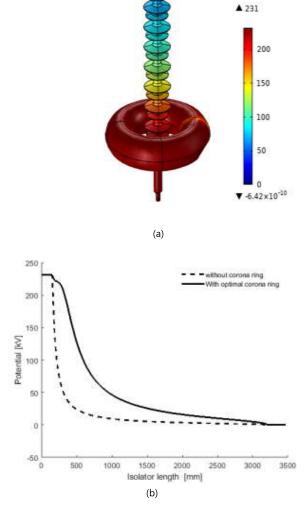

(a)

(b)

FIGURE 13. Electric potential along the composite insulator a)On the surfaces of the composite insulator and the corona ring b)Electric potential along the insulator without and with optimal corona ring.

self-cancellation field created by the ring and one created on insulators' surface.

The use of an optimized corona ring enhances the distribution of the electric field (tangential) on the insulator surface. As a result, its amplitude is reduced by almost 82%, especially on the VH side. In addition, the installation of a corona ring allows obtaining a more uniform distribution of the voltage as illustrated in Figure 13.

VI. CONCLUSION
In this paper, a multi-objective optimization problem giving the electric field norm as function of the corona ring parameters (consisting in its radius, the radius of its tube, and its vertical position concerning the HV terminal) over 400 kV composite type insulator string is established. To achieve this problem, three powerful multi-objective algorithms MOALO, MOPSO and NSGA-II are developed. The proposed algorithms solved the problem successfully, proving their applicability and computational efficiency.

Furthermore, the optimization study for three objectives optimization was carried out, and the results showed that MOPSO gives much better distribution solutions over the non-dominated front. However, MOALO allows obtaining a reduction of about 55% and 75% in computational time, compared to those taken while executing the MOPSO and the NSGA-II, respectively.

In the presence of the corona ring optimized parameters configuration, the magnitude of the electric field in the triple point was decreased of about 95% compared to without corona ring, and even the electric field value along the surface of the insulator sheds and flange (1.3kV/cm on the insulator sheds), is well below the maximum electric field recommended values. In addition, an improvement of about 38% in the voltage distribution is noted.

ACKNOWLEDGMENT

REFERENCES

[1] B. M'hamdi, M. Teguar, and A. Mekhaldi, "Potential and electric field distributions on HV insulators string used in the 400 kV novel transmission line in Algeria," in *Proc. IEEE Int. Conf. Solid Dielectrics (ICSD)*, Jun. 2013, pp. 190–193.

[2] D. Doufene, S. Bouazabia, and A. Haddad, "Optimised performance of cap and pin insulator under wet pollution conditions using a mono-objective genetic algorithm," *Austral. J. Electr. Electron. Eng.*, vol. 16, no. 3, pp. 149–162, Jul. 2019.

[3] D. Doufene, S. Bouazabia, and A. Haddad, "Shape and electric performance improvement of an insulator string using particles swarm algorithm," *IET Sci., Meas. Technol.*, vol. 14, no. 2, pp. 198–205, Mar. 2020.

[4] S. Zhang, Z. Peng, L. Peng, and H. Wang, "Optimization of corona ring structure for UHV composite insulator using finite element method and PSO algorithm," in *Proc. IEEE Int. Conf. Solid Dielectr. (ICSD)*, Jun. 2013, pp. 210–213.

[5] M. A. F. Rosli, N. M. B. Sham, M. S. Kamarudin, M. F. M. Yousof, N. A. M. Jamail, and R. A. Rahman, "The effectiveness of mitigation schemes on electric field intensity (stress control) for overhead line glass insulator," *Int. J. Electr. Electron. Eng. Telecommun.*, vol. 11, no. 1, pp. 12–17, Jan. 2022.

[6] G. Shanmugam and S. Karakkad, "Influence of the insulator geometry on the streamer propagation characteristics in polymeric insulators under positive polarity lightning impulse voltages," *IET Sci., Meas. Technol.*, vol. 12, no. 8, pp. 1082–1088, Nov. 2018.

[7] E. D. S. Domingues, "Improved condition monitoring of composite insulators," Ph.D. dissertation, Univ. Manchester, Manchester, U.K., 2012.

[8] M. Bouhaouche, M. Teguar, and A. Mekhaldi, "Improvement of electric field distribution by integrating composite insulators in a 400 kV AC double circuit line in Algeria," *IEEE Trans. Dielectr. Electr. Insul.*, vol. 24, no. 6, pp. 861–867, Dec. 2017.

[9] W.-D. Li, X.-R. Li, B.-H. Guo, C. Wang, Z. Liu, and G.-J. Zhang, "Topology optimization of truncated cone insulator with graded permittivity using variable density method," *IEEE Trans. Dielectr. Electr. Insul.*, vol. 26, no. 1, pp. 1–9, Feb. 2019.

[10] A. J. Phillips, A. J. Maxwell, C. S. Engelbrecht, and I. Gutman, "Electric-field limits for the design of grading rings for composite line insulators," *IEEE Trans. Power Del.*, vol. 30, no. 3, pp. 1110–1118, Jun. 2015.

[11] J. Wang, B. Yue, X. Deng, T. Liu, and Z. Peng, "Electric field evaluation and optimization of shielding electrodes for high voltage apparatus in ±1100 kV indoor DC yard," *IEEE Trans. Dielectr. Electr. Insul.*, vol. 25, no. 1, pp. 321–329, Feb. 2018.

[12] J. He and R. S. Gorur, "Charge simulation based electric field analysis of composite insulators for HVDC lines," *IEEE Trans. Dielectr. Electr. Insul.*, vol. 21, no. 6, pp. 1638–1646, Dec. 2014.

[13] J. Du, Z. Peng, J. Li, S. Zhang, N. Li, and C. Fan, "Electric field calculation and grading ring optimization for 1000 kV AC post porcelain insulator," in *Proc. IEEE Int. Conf. Solid Dielectr. (ICSD)*, Bologna, Italy, Jun. 2013, pp. 198–201.

[14] T. Doshi, R. Gorur, and J. Hunt, "Electric field computation of composite line insulators up to 1200 kV AC," *IEEE Trans. Dielectr. Electr. Insul.*, vol. 18, no. 3, pp. 861–867, Jun. 2011.

[15] B. M'hamdi, M. Teguar, and A. Mekhaldi, "Optimal design of corona ring on HV composite insulator using PSO approach with dynamic population size," *IEEE Trans. Dielectr. Electr. Insul.*, vol. 23, no. 2, pp. 1048–1057, Apr. 2016.

[16] N. Alti, A. Bayadi, and K. Belhouchet, "Grading ring parameters optimization for 220 kV meta-oxide arrester using 3D-FEM method and bat algorithm," *IET Sci., Meas. Technol.*, vol. 15, no. 1, pp. 14–24, Jan. 2021.

[17] K. Aramugam, H. A. Illias, and Y. C. Ching, "Optimisation of corona ring design for composite insulator strings," *Int. J. Comput. Math. Electr. Electron. Eng.*, vol. 38, no. 1, pp. 232–246, 2019.

[18] J. A. Diaz-Acevedo, A. Escobar, and L. F. Grisales-Noreña, "Optimization of corona ring for 230 kV polymeric insulator based on finite element method and PSO algorithm," *Electric Power Syst. Res.*, vol. 201, Dec. 2021, Art. no. 107521.

[19] S. Mirjalili, P. Jangir, and S. Saremi, "Multi-objective ant lion optimizer: A multi-objective optimization algorithm for solving engineering problems," *Appl. Intell.*, vol. 46, no. 1, pp. 79–95, Jan. 2017.

[20] M. Mitchell, *An Introduction to Genetic Algorithms*. Cambridge, U.K.: MIT Press, Jan. 1998.

[21] M. Dorigo, V. Maniezzo, and A. Colorni, "Ant system: Optimization by a colony of cooperating agents," *IEEE Trans. Syst., Man, Cybern., B (Cybernetics)*, vol. 26, no. 1, pp. 29–41, Feb. 1996.

[22] J. Kennedy and R. Eberhart, "Particle swarm optimization," in *Proc. Int. Conf. Neural Netw.*, Dec. 1995, pp. 1942–1948.

[23] X. S. Yang, *Cuckoo Search and Firefly Algorithm: Theory and Applications* (Studies in Computational Intelligence). Cham, Switzerland: Springer, 2014.

[24] S. Mirjalili and A. Lewis, "The whale optimization algorithm," *Adv. Eng. Softw.*, vol. 95, pp. 51–67, Jan. 2016.

[25] S. Mirjalili, S. M. Mirjalili, and A. Lewis, "Grey wolf optimizer," *Adv. Eng. Softw.*, vol. 69, pp. 46–61, Jan. 2014.

[26] S. Mirjalili, "The ant lion optimizer," *Adv. Eng. Softw.*, vol. 83, pp. 80–98, May 2015.

[27] M. D. Li, H. Zhao, X. W. Weng, and T. Han, "A novel nature-inspired algorithm for optimization: Virus colony search," *Adv. Eng. Softw.*, vol. 92, pp. 65–88, Feb. 2016.

[28] A. Kaveh and N. Farhoudi, "A new optimization method: Dolphin echolocation," *Adv. Eng. Softw.*, vol. 59, pp. 53–70, May 2013.

[29] H. Benguesmia, N. M'ziou, and A. Boubakeur, "Simulation of the potential and electric field distribution on high voltage insulator using the finite element method," *Diagnostyka*, vol. 19, no. 2, pp. 41–52, 2018.

[30] K. Deb, A. Pratap, S. Agarwal, and T. Meyarivan, "A fast elitist non-dominated sorting genetic algorithm: NSGA-II," *IEEE Trans. Evol. Comput.*, vol. 6, no. 2, pp. 182–197, Apr. 2002.

[31] J. Moore and R. Chapman, "Application of particle swarm to multiobjective optimization," Dept. Comput. Sci. Softw. Eng., Auburn Univ., Auburn, AL, USA, Tech. Rep., vol. 32, 1999.

[32] C. A. C. Coello, D. A. V. Veldhuizen, and G. B. Lamont, *Evolutionary Algorithms for Solving Multi-Objective Problems*, 2nd ed. New York, NY, USA: Kluwer, 2007, pp. 1–19.

BENALIA M'HAMDI received the Ingénieur d'Etat degree from the University of Sidi Belabes, Algeria, in 1991, the Magister degree, in 2007, and the Ph.D. degree in high voltage engineering from the Polytechnic of Algiers, Algeria (ENP), in 2016. His research interests include high voltage technology, outdoor insulation, optimization problems, and artificial intelligence.

YOUCEF BENMAHAMED (Member, IEEE) received the engineer's and master's degrees in power electronics engineering, in 2014, and the Ph.D. degree in high voltage techniques from the École Nationale Polytechnique (ENP), Algiers, in 2019. His research interests include diagnosis, artificial intelligence, and optimization techniques.

IBRAHIM B. M. TAHA received the B.Sc. degree from the Faculty of Engineering at Tanta, Tanta University, Egypt, in 1995, the M.Sc. degree from the Faculty of Engineering at Mansoura, Mansoura University, Egypt, in 1999, and the Ph.D. degree in electrical power and machines from the Faculty of Engineering, Tanta University, in 2007. Since 1996, he has been teaching at the Faculty of Engineering, Tanta University. He joined Taif University as an Assistant Professor with the Electrical Engineering Department, Faculty of Engineering. His research interests include steady state and transient stability of HVDC systems, FACTS, multilevel inverters, dissolved gas analysis, and AI technique applications.

MADJID TEGUAR received the degree in electrical engineering in 1990, the master's degree, in 1993, and the Ph.D. degree in high voltage engineering from Ecole Nationale Polytechnique (ENP), Algiers, in 2003. He is currently a Professor of electrical engineering with ENP. His research interests include insulation systems, insulation coordination, earthing of electrical energy systems, and polymeric cables insulation.

SHERIF S. M. GHONEIM (Senior Member, IEEE) received the B.Sc. and M.Sc. degrees from the Faculty of Engineering at Shoubra, Zagazig University, Egypt, in 1994 and 2000, respectively, and the Ph.D. degree in electrical power and machines from the Faculty of Engineering, Cairo University, in 2008. Since 1996, he has been teaching at the Faculty of Industrial Education, Suez Canal University, Egypt. From 2005 to 2007, he was a Guest Researcher at the Institute of Energy Transport and Storage (ETS), University of Duisburg–Essen, Germany. He joined Taif University as an Associate Professor with the Electrical Engineering Department, Faculty of Engineering. His research interests include grounding systems, dissolved gas analysis, breakdown in SF_6 gas, and AI technique applications.

$\bullet\bullet\bullet$